GEOPHYSICAL RESEARCH LETTERS, VOL. 34, L08307, doi:10.1029/2007GL029250, 2007

A constitutive model for layer development in shear zones near the brittle-ductile transition

Laurent G. J. Montési[1]

Received 15 January 2007; revised 16 March 2007; accepted 26 March 2007; published 27 April 2007.

[1] The microstructure of ductile shear zones differs from that of surrounding wall rocks. In particular, compositional layering is a hallmark of shear zones. As layered rocks are weaker than their isotropic protolith when loaded in simple shear, layering may hold the key to explain localization of ductile deformation onto ductile shear zones. I propose here a constitutive model for layer development. A two-level mixing theory allows the strength of the aggregate to be estimated at intermediate degrees of layering. A probabilistic failure model is introduced to control how layers develop in a deforming aggregate. This model captures one of the initial mechanism of phase interconnection identified experimentally by Holyoke and Tullis (2006a, 2006b), fracturing of load bearing grains. This model reproduces the strength evolution of these experiments and can now be applied to tectonic modeling.
Citation: Montési, L. G. J. (2007), A constitutive model for layer development in shear zones near the brittle-ductile transition, *Geophys. Res. Lett.*, *34*, L08307, doi:10.1029/2007GL029250.

1. Introduction

[2] The formation of ductile shear zones is a long-standing enigma of geodynamics. Laboratory experiments indicate that high temperature or pressure generally prevent localization of deformation, producing distributed, or ductile, deformation instead [*Evans et al.*, 1990]. By contrast, natural deformation remains localized even at conditions that lead to distributed deformation in the laboratory [*Rutter et al.*, 2001; *Vauchez and Tommasi*, 2003].

[3] A likely explanation for this difference in deformation style between laboratory and natural deformation lies in the microstructure of shear zones. Reduced grain size, crystallographic preferred orientation, greater abundance and interconnection of phyllosilicates are often associated with shear zones [*White et al.*, 1980; *Gueydan et al.*, 2003]. Compositional layering, which is a type of foliation, is particularly common in middle to lower continental crust shear zones. It facilitates shearing along these layers and weakens the shear zone rocks significantly. I propose here a constitutive model to capture the development of this type of foliation in a deforming polyphase aggregate and the accompanying weakening.

[4] This model is inspired by laboratory experiments in which interconnection of the weak phase occurs through brittle fracture of stronger framework grains [*Holyoke and Tullis*, 2006a, 2006b]. Field studies in which clasts of protolith are observed in the phyllosilicate-rich matrix of natural shear zones [*Jefferies et al.*, 2006] or in which brittle precursors are seen to control shear zone geometry [*Gueydan et al.*, 2003; *Mancktelow and Pennacchioni*, 2005] indicate that this mechanism is active in nature. Below, I describe how to estimate rock strength when layering is partially developed, present a probabilistic failure model that captures the initial interconnection process identified in the experiments of *Holyoke and Tullis* [2006a, 2006b], and compare the strength evolution predicted by this model with the evolution observed experimentally.

2. Aggregate Strength

[5] As the kinematics of shear zones are dominated by simple shear deformation, only one strain rate, $\dot{\varepsilon}$, and one stress, σ, need to be considered. At the temperature and pressure of the middle to lower crust, an aggregate of phase i is assumed to obey a power law rheology

$$\dot{\varepsilon} = B_i \sigma^{n_i}, \tag{1}$$

where n_i and B_i are the stress exponent and strength factor appropriate for material i. The latter depends on a variety of parameters, among which only temperature appears explicitly here, through

$$B_i = A_i \exp(Q_i/RT), \tag{2}$$

where A_i and Q_i are the pre-exponential factor and activation energy, respectively, and R is the gas constant.

[6] The strength of a polymineralic aggregate can be related conceptually to the rheology of its component phases using a mixture model [*Hill*, 1963; *Handy*, 1994; *Ji et al.*, 2003]. While accurate strength estimates need to consider the detailed microstructure of the aggregate [*Handy*, 1990; *Tullis et al.*, 1991], useful constraints can be gleaned by considering the simple constant strain rate and constant stress approximations.

[7] When the strongest phase forms a load-bearing framework, the strain rate $\dot{\varepsilon}_d$ is uniform throughout the rock. The strength of the aggregate is then the average of stress required for each phase to deform at $\dot{\varepsilon}_d$, weighted by the volume fraction of each phase, ϕ_i

$$\sigma_d = \sum_i \phi_i (\dot{\varepsilon}_d / B_i)^{1/n_i}. \tag{3}$$

This relation is used to describe the undeformed protolith.

[8] However, in a layered rock, each phase is interconnected, implying that the shear stress parallel to the layers is continuous throughout the aggregate. The strain

[1]Department of Marine Geology and Geophysics, Woods Hole Oceanographic Institution, Woods Hole, Massachusetts, USA.

0094-8276/07/2007GL029250$05.00

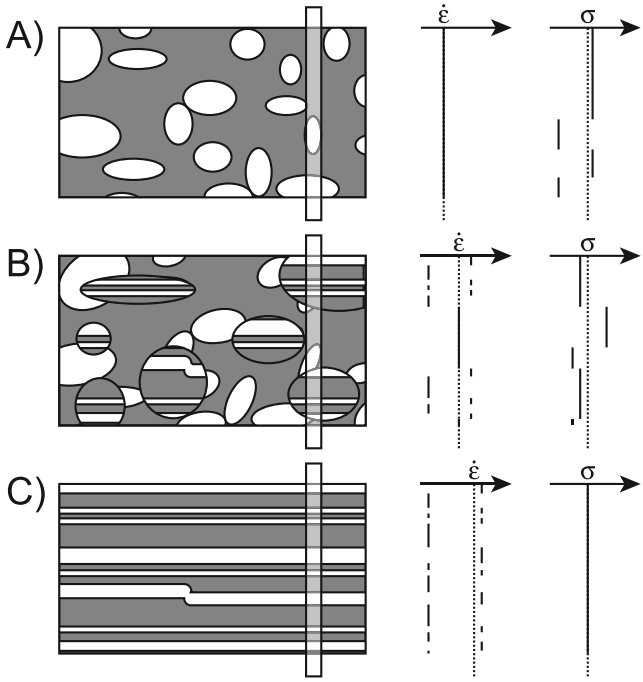

Figure 1. Conceptual models used to estimate the strength of a polyphase aggregate in which the component phases are (a) dispersed throughout the aggregate (protolith), (b) locally connected, and (c) fully interconnected (layered structure). The stronger phase is shaded while the weaker phase is in white. Schematic strain rate ($\dot{\varepsilon}$) and stress (σ) profiles, corresponding to the area outlined by a translucent white box, are reported to the right of each diagram along with the average value as a dotted line. In Figure 1a, strain rate is constant while in Figure 1c, stress is constant throughout the aggregate. Layering occurs initially in patches distributed throughout the sample (Figure 1b).

rate is then the average of that in each component, weighted by ϕ_i

$$\dot{\varepsilon}_c = \sum_i \phi_i \, B_i \, \sigma_c^{n_i}. \tag{4}$$

The layered rock is usually weaker than the protolith.

[9] The transition from dispersed to layered microstructure occurs in patches throughout the aggregate [*Holyoke and Tullis*, 2006a, 2006b]. The location of each patch depends on local stress concentration but I assume here for simplicity that these patches occur randomly throughout the aggregate. Thus, when layering is incomplete, layered patches can be regarded as a weak pseudophase dispersed throughout a matrix of stronger protolith (Figure 1b).

[10] The layered pseudophase obeys equation (4) and occupies a volume fraction f while the protolith pseudophase obeys equation (3) and occupies a volume fraction $1 - f$. Then, the strength of the aggregate can be estimated by mixing at constant strain rate the strength of these two pseudophases, giving

$$\sigma = (1 - f)\, \sigma_d + f\, \sigma_c. \tag{5}$$

[11] The stress in the protolith fraction, σ_d, can be expressed as a function of the stress in the foliated fraction, σ_c, by substituting equation (4) into equation (3). Then, the stress supported by the entire aggregate is given by

$$\frac{\sigma}{\sigma_c} = f + (1 - f) \sum_j \phi_j \left[\sum_i \phi_i \, B_i \, B_j^{-1} \sigma_c^{n_i - n_j} \right]^{1/n_j}, \tag{6}$$

which, together with equation (4), provides an implicit way to calculate the stress-strain rate relation of a partially foliated aggregate.

[12] In most applications, it is sufficient to assume that only two phases are present. In this case, equation (6) becomes

$$\frac{\sigma}{\sigma_c} = f + (1 - f)(1 - \phi_b) \left[(1 - \phi_b) + \phi_b \frac{B_b \sigma_c^{n_b}}{B_a \sigma_c^{n_a}} \right]^{1/n_a} + (1 - f)\phi_b \left[\phi_b + (1 - \phi_b) \frac{B_a \sigma_c^{n_a}}{B_b \sigma_c^{n_b}} \right]^{1/n_b}. \tag{7}$$

[13] This two-level mixing model looses its validity at high abundance of weak phase and/or degree of layering f, although the limits $f \to 1$ and $C \to 1$ are correct. A more advanced model would account for the fact that as the strong phase (or protolith pseudophase) becomes rare, it looses its load-bearing characteristics and behaves instead as strong clasts or boudins in a weak medium [*Handy*, 1990].

[14] As layers develop, the strength of the aggregate changes from being dominated by the strong phase to being dominated by the weak phase (Figure 2). The change requires a higher degree of layering f for a higher strength contrast between the end-member phases (Figure 2) and is more sudden at a small fraction of weak phase. Thus, the formation of layers is a highly efficient weakening mechanism in rocks that include a small fraction of a weak phase.

3. Microstructure Evolution

[15] Layering develops progressively with strain due to a combination of grain rotation, shearing, and failure. While rotation and shearing may dominate at high temperature, initial layer development is controlled by failure of load-bearing grains in some of the experiments of *Holyoke and Tullis* [2006a, 2006b]. To capture this phenomenon, I propose the following probabilistic failure model.

[16] Suppose that an external stress σ is applied to the aggregate. The local stress at grain intersections, s, differs in general from the external stress. Overall, the stress is enhanced by a factor E. Furthermore, variability in grain contact environment leads to a distribution of local stress s that, in the absence of more specific information, I take to be Gaussian with variance ξ. Therefore, the probability that the stress at any given grain intersection is s under the external stress σ follows

$$p(s|\sigma) = \frac{1}{\xi\sqrt{2}} \exp\left[-\frac{(s - E\sigma)^2}{2\xi^2} \right]. \tag{8}$$

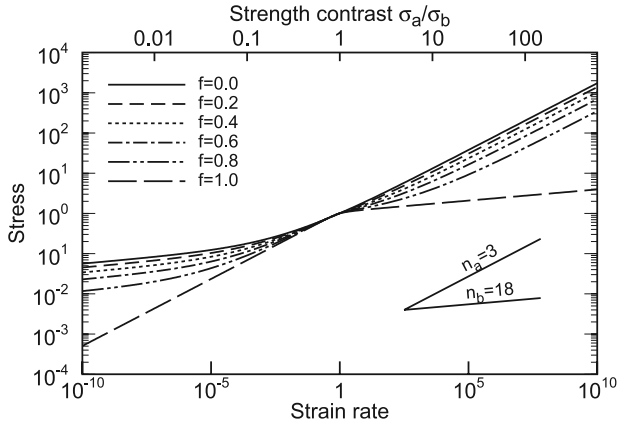

Figure 2. Stress/strain rate relations for an aggregate that includes 20% of a phase *b* for various degrees of layering, *f*. The stress supported by each phase is 1 at a strain rate of 1, but the different stress exponents of the constituent phases imply that phase *b* is weaker when the strain rate is more than 1 and vice versa (top axis).

[17] If grain scale failure occurs when the local stress exceeds a yield strength s_y, the fraction of sites at failure is given by

$$N(\sigma) = \int_{s_y}^{+\infty} p(s|\sigma)ds = \frac{1}{2}\left[1 + \mathrm{erf}\left(\frac{\sigma - \sigma_y}{\chi\sqrt{2}}\right)\right], \qquad (9)$$

with $\sigma_y = s_y/E$ and $\chi = \xi/E$ the equivalent macroscopic yield strength and stress variance (Figure 3).

[18] Among the sites undergoing failure, $N(1 - f)$ are located in a non-foliated portion of the aggregate. Only in these sites can failure increase the overall layering. Introducing a rate constant λ, the fraction of the aggregate with layered microstructure, *f*, evolves as

$$\frac{df}{d\varepsilon} = \frac{1}{\lambda}(1 - f)\ \frac{1}{2}\left[1 + \mathrm{erf}\left(\frac{\sigma - \sigma_y}{\chi\sqrt{2}}\right)\right] \qquad (10)$$

[19] A similar failure model has been proposed to describe cataclastic flow of porous sandstones. Acoustic emissions, which reflect microcracking, are approximately normally distributed around a yield point. This lends credence to the Gaussian microstress distribution assumed here [*Zhu*, 2006]. The decrease of permeability upon cataclastic failure, which represents the integrated damage, follows approximately an error function with the applied stress (W. Zhu et al., A probabilistic damage model of stress-induced permeability anisotropy during cataclastic flow, submitted to *Journal of Geophysical Research*, 2006).

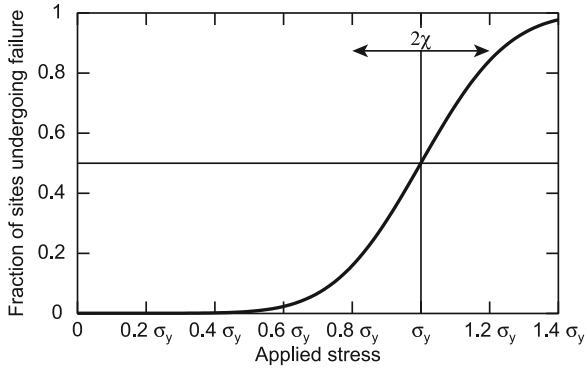

Figure 3. Fraction of microscopic sites undergoing failure as a function of applied stress scaled by the apparent failure strength σ_y. In this plot, the local stresses variance is $\chi = 0.2\sigma_y$.

4. Comparison With Laboratory Experiments

[20] As this model is inspired by the experiments of *Holyoke and Tullis* [2006a, 2006b], it is important to evaluate how well it captures the stress-strain curves of these studies. In these experiments, a thin sample of a natural polyphase aggregate is loaded under general shear. The loading configuration is idealized as a linear elastic spring with stiffness *K* such that

$$d\sigma/dt = K\left(\dot{\varepsilon}_p - \dot{\varepsilon}\right), \qquad (11)$$

where $\dot{\varepsilon}_p$ is the load point velocity.

[21] To simulate Holyoke and Tullis's experiments, equations (4), (5), (10), and (11) are integrated under constant $\dot{\varepsilon}_p$ with initial conditions $\sigma = 0$ and $f = 0$.

[22] The stress initially increases as the strain rate of the aggregate is much less than the loading velocity. That portion of the stress-strain curves is essentially linear, with slope *K*.

[23] In these simulations, The sample subsequently yields at a stress not exceeding that of the non-foliated protolith. As the stress reaches approximately $\sigma_y - \chi$, layers starts to develop, accompanied by weakening of the sample. Weakening is sometimes so severe that layering ceases to increase as few microscopic sites have sufficient stress for failure. Conversely, if $\sigma_y - \chi$ is low, the peak strength may be

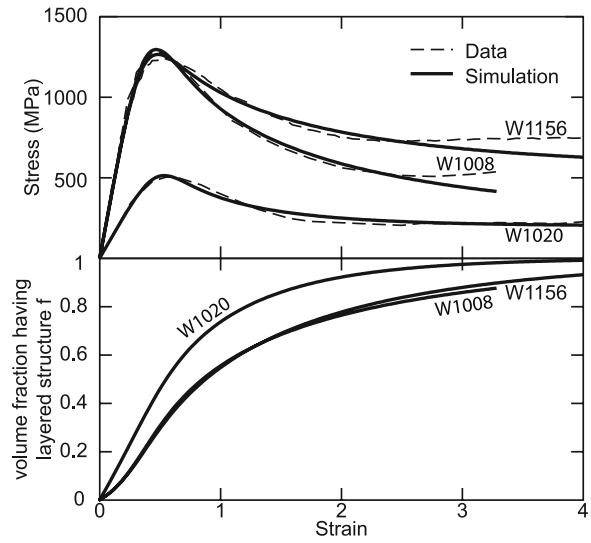

Figure 4. Comparison between numerical simulations (solid lines) and three laboratory experiments on Gneiss minuti by *Holyoke and Tullis* [2006a, 2006b]. Top: strength evolution; Bottom: progression of the volume fraction of rock having a layered structure *f* inferred from the simulations. Experimental conditions and fit parameters are reported in Table 1.

significantly less than that of the protolith as considerable layer formation can occur even during the elastic loading stage (Figure 4).

[24] *Holyoke and Tullis* [2006a, 2006b] tested a Gneiss Minuti composed of feldspar, quartz, and 13% biotite. For simplicity, I consider only two phases and adjust the strength of each phase, B_a and B_b, as well as the evolution rate constant λ to fit the experimental stress-strain curves (Table 1). The stress exponent of the weak phase is fixed to $n_b = 18$, like biotite [*Kronenberg et al.*, 1990], while that of the strong phase is $n_a = 3$, like quartz or feldspar [*Kohlstedt et al.*, 1995]. The simulations are not very sensitive to n_a but n_b and λ combine to control the sharpness of the weakening.

[25] *Holyoke and Tullis* [2006a, 2006b] conducted their experiments at two different temperatures and two strain rates (Table 1). It is possible to obtain a good fit to the experiments with a unique σ_y and χ. The exact value of these parameters is poorly constrained but $\sigma_y - \chi \sim 500$MPa.

[26] The simulations of Figure 4 use the parameters in Table 1. Several combinations of parameters entering the constitutive models give comparable fits, preventing rigorous inversion of experimental data. However, such inversion might be misleading as the proposed model does not capture all the actual phenomena active in the experiment, such as intracrystalline hardening and syndeformation metamorphism [*Holyoke and Tullis*, 2006b, 2006c].

[27] The preferred values of B_a and B_b need to vary only with temperature. For the strong phase, such a variation corresponds to an activation energy of $Q_a = 250$ kJ/mol comparable to that of quartz and feldspar. A similar interpretation for the weak phase would imply $Q_b = 3000$ kJ/mol well in excess of published value for biotite [*Kronenberg et al.*, 1990; *Mariani et al.*, 2006]. Instead, the change in B_b with temperature probably reflects the appearance of reaction products [*Holyoke and Tullis*, 2006c] that take over the role of biotite as the weak phase in the high-temperature experiments. No reaction was observed in the low-temperature samples [*Holyoke and Tullis*, 2006c].

[28] The λ factor indicates more sluggish microstructure evolution in experiment W1020. λ appears roughly proportional to applied stress. The origin of this variation needs to be investigated in more detail.

5. Outlook

[29] The model proposed here captures the strength evolution of the experiments of *Holyoke and Tullis* [2006a, 2006b]. It can now be applied to lithosphere-scale deformation. For that purpose, one needs to specify the rheologies of each mineral end-member and three additional parameters: the yield strength σ_y, possibly linked to the macroscopic brittle failure criterion, the local stress variance χ, and the rate constant λ. According to this study, χ is comparable, although smaller, to σ_y. The λ parameter is the least understood. Values between 1 and 10 provide good matches to laboratory experiments. It may be proportional to stress.

[30] With this formulation, layering develops only in a relatively strong protolith close to the brittle-ductile transition. At higher temperature, grain rotation and shearing may become the dominant mechanism for forming layers. The high-temperature regime is not included in this model.

Table 1. Experimental Conditions From *Holyoke and Tullis* [2006b] and Fit Parameters for the Data in Figure 4

	W1156	W1008	W1020
Temperature, °C	745	800	800
Strain rate,s^{-1}	1.9×10^{-6}	1.3×10^{-5}	1.3×10^{-6}
n_a	3	3	3
n_b	18	18	18
σ_y, MPa	2000	2000	2000
χ, MPa	1500	1500	1500
B_a, MPa	1700[a]	1984[a]	904[a]
B_b, MPa	500[b]	203[b]	178[b]
$1/\lambda$	3.1	3.2	9.5
K, MPa	4027	4047	1297

[a] $A_a = 3.867 \times 10^{-6}$MPa^{-3}s^{-1}, $Q_a = 250$ kJ/mol.
[b] $A_b = 4.981 \times 10^{-55}$MPa^{-3}s^{-1}, $Q_b = 3000$ kJ/mol (apparent value reflecting reaction (see text)).

[31] In addition to providing a means of interconnecting weak phases, grain failure also leads to new fluid pathways through the rock and produces new grain surfaces. These effects enhance fluid-rock reactions, further weakening the aggregate [*Gueydan et al.*, 2003; *Holyoke and Tullis*, 2006a, 2006c]. *Gueydan et al.* [2004] show how such reactions can result in lithosphere-scale shear zones. It should also be noted that the strength model presented here does not require that each layer has a specific composition: layering could be defined by grain size or mineral orientation.

[32] Finally, deformation in the lithosphere is not necessarily restricted to simple shear. The weakening described here affects only the components of the stress tensor resolved on the layers. Weakening is anisotropic, favoring simple shear deformation. Furthermore, the strength of mica is strongly anisotropic [*Kronenberg et al.*, 1990; *Mares and Kronenberg*, 1993], so that crystal alignment that follows phase interconnection described here also weakens the shear zone when loaded in simple shear. Anisotropic weakening may be the key to predicting the asymmetry observed in lithosphere-scale simple shear deformation such as core complexes, half graben, and one-sided subduction.

[33] **Acknowledgments.** I thank Frédéric Gueydan, Caleb Holyoke, Andreas Kronenberg, and Associate Editor Éric Calais, for their reviews and Mark Jessell for an invitation to the 2006 Gordon Research Conference on Rock Deformation. This project was supported by NSF grant EAR-0337678 and the Andrew W. Mellon Foundation Endowed Fund for Innovative Research.

References

Evans, B., J. T. Fredrich, and T. f. Wong (1990), The brittle-ductile transition in rocks: Recent experimental and theoretical progress, in *The Brittle-Ductile Transition in Rocks*, *Geophys. Monogr. Ser.*, vol. 56, edited by A. G. Duba et al., pp. 1–20, AGU, Washington, D. C.

Gueydan, F., Y. M. Leroy, L. Jolivet, and P. Agard (2003), Analysis of continental midcrustal strain localization induced by microfracturing and reaction-softening, *J. Geophys. Res.*, *108*(B2), 2064, doi:10.1029/2001JB000611.

Gueydan, F., Y. M. Leroy, and L. Jolivet (2004), Mechanics of low-angle extensional shear zones at the brittle-ductile transition, *J. Geophys. Res.*, *109*, B12407, doi:10.1029/2003JB002806.

Handy, M. R. (1990), The solid-state flow of polymineralic rocks, *J. Geophys. Res.*, *95*(B6), 8647–8661.

Handy, M. R. (1994), Flow laws for rocks containing two non-linear viscous phases: A phenomenological approach, *J. Struct. Geol.*, *16*, 287–301.

Hill, R. (1963), Elastic properties of reinforced solids: Some theoretical principles, *J. Mech. Phys. Solids*, *11*, 357–372.

Holyoke, C. W., III, and J. Tullis (2006a), Formation and maintenance of shear zones, *Geology*, *34*, 105–108, doi:10.1130/GC22116.1.

Holyoke, C. W., III, and J. Tullis (2006b), Mechanisms of weak phase interconnection and the effects of phase strength contrast on fabric development, *J. Struct. Geol.*, *28*, 621–640.

Holyoke, C. W., III, and J. Tullis (2006c), The interaction between reaction and deformation: An experimental study using a biotite + plagioclase + quartz gneiss, *J. Metamorph. Geol.*, *24*, 743–762, doi:10.1111/j.1525-1314.2006.00666.x.

Jefferies, S., R. Holdsworth, C. Wibberley, T. Shimamoto, C. Spiers, A. Niemeijer, and G. Lloyd (2006), The nature and importance of phyllonite development in crustal-scale fault cores: An example from the Median Tectonic Line, Japan, *J. Struct. Geol.*, *28*, 220–235.

Ji, S., P. Shao, and B. Xia (2003), Flow laws of multiphase materials and rocks from end-member flow laws, *Tectonophysics*, *370*, 129–145, doi:10.1016/S0040-1951(03)001823.

Kohlstedt, D. L., B. Evans, and S. J. Mackwell (1995), Strength of the lithosphere: Constraints imposed by laboratory experiments, *J. Geophys. Res.*, *100*(B9), 17,587–17,602.

Kronenberg, A. K., S. L. Kirby, and J. Pinkston (1990), Basal slip and mechanical anisotropy of biotite, *J. Geophys. Res.*, *95*(B12), 19,257–19,278.

Mancktelow, N. S., and G. Pennacchioni (2005), The control of precursor brittle fracture and fluid-rock interaction on the development of single and paired ductile shear zones, *J. Struct. Geol.*, *27*, 645–661.

Mares, V. M., and A. K. Kronenberg (1993), Experimental deformation of muscovite, *J. Struct. Geol.*, *15*, 1061–1075.

Mariani, E., K. H. Brodie, and E. H. Rutter (2006), Experimental deformation of muscovite shear zones at high temperatures under hydrothermal conditions and the strength of phyllosilicate-bearing faults in nature, *J. Struct. Geol.*, *28*, 1569–1587.

Rutter, E. H., R. E. Holdsworth, and R. J. Knipe (2001), The nature and tectonic significance of fault-zone weakening: An introduction, *Geol. Soc. Spec. Publ.*, *186*, 1–11.

Tullis, T. E., F. G. Horowitz, and J. Tullis (1991), Flow laws of polyphase aggregates from end-member flow laws, *J. Geophys. Res.*, *96*(B5), 8081–8096.

Vauchez, A., and A. Tommasi (2003), Wrench faults down to the asthenosphere: Geological and geophysical evidence and thermo-mechanical effects, *Geol. Soc. Spec. Publ.*, *210*, 15–34.

White, S. H., S. E. Burrows, J. Carreras, N. D. Shaw, and F. J. Humphreys (1980), On mylonites in ductile shear zones, *J. Struct. Geol.*, *2*, 175–187.

Zhu, W. (2006), Quantitative characterization of permeability reduction associated with compactive cataclastic flow, in *Radiated Energy and the Physics of Earthquake Faulting*, *Geophys. Monogr. Ser.*, vol. 170, edited by R. Abercrombie et al., pp. 143–151, AGU, Washington, D. C.

L. G. J. Montési, Department of Marine Geology and Geophysics, Woods Hole Oceanographic Institution, MS 24, Woods Hole, MA 02543, USA. (montesi@whoi.edu)